ELM suppression through modification of Edge Profiles with Lithium Wall Coatings in NSTX

R. Maingi[a], T.H. Osborne[b], J.M. Canik[a], J. Manickam[c], and the NSTX research team

[a]*Oak Ridge National Laboratory, Oak Ridge TN, 37831 USA*

[b]*General Atomics, San Diego, CA, 92121 USA*

[c]*Princeton Plasma Physics Laboratory, Princeton, NJ 08543 USA*

Presenting author email: rmaingi@pppl.gov

Lithium (li) coatings were employed in the National Spherical Torus Experiment (NSTX) to reduce recycling and provide density control[1]. These coatings also improve energy confinement, mainly through reduction of the core electron transport[2, 3]. When 'thick' coatings were applied between discharges, edge localized modes (ELMs) were completely suppressed[4]. With coatings of 'intermediate thickness', the phenomenology of ELM suppression was made clear: they were suppressed gradually via growing periods of quiescence. The final post-lithium discharges were ELM-free with a 50% increase in normalized energy confinement, up to the global β_N ~ 5.5-6 limit where resistive wall modes limited the operational space[5, 6].

The measured edge profiles in both the pre-li and final ELM-free post-li discharges were simulated with the SOLPS code package[7] to quantify the changes in the recycling and edge transport rates[8]. The experimental observations[5, 6] are summarized here: the edge n_e profile gradients inside the separatrix were reduced with li wall coatings, due partly to lower recycling and edge fueling, which effectively shifted the density profile inward by up to 2-3 cm. In contrast, the edge T_e profile was unaffected in the H-mode pedestal steep gradient region at constant plasma stored energy; however, the region of steep gradients extended radially inward by several cm following li coatings.

The midplane n_e, T_e, and T_i profiles were used to constrain the radial profiles of the cross-field particle and electron/ion thermal diffusivity (D, χ_e, χ_i), which were assumed to be

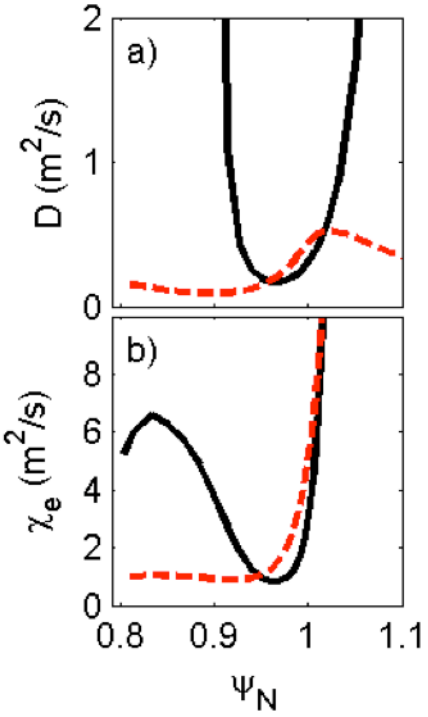

Fig. 1 – Comparison of computed a) particle and b) electron thermal diffusivity for pre-li (solid black - #129015) and post-li (dashed red - #129038) discharges.

constant on flux surfaces. The divertor D_α emission profile was used to evaluate the change in the recycling coefficient, and the divertor heat flux profile was used to constrain the power balance. One additional input variation was required: the power flowing into the scrape-off layer was ~ 50% lower in the post-li discharge, in line with the programmed reduction in the NBI power.

The SOLPS modeling indicated[8] a divertor recycling coefficient reduction from 0.98 to ~ 0.90 to reproduce the observed drop in divertor D_α. However the calculated post-li n_e, T_e, and T_i profiles did not match the measured profiles with the same D, χ_e, and χ_i profiles used in the pre-li discharges; indeed, the computed profile gradients were larger than the measured ones. Hence a reduction in both the recycling coefficient *and* a drop in the edge and SOL cross-field transport coefficients was required to match the post-lithium profiles.

The 'best fit' coefficients for the pre-li and post-li profiles are compared in Figure 1. In the steep gradient region between ψ_N of ~0.95 and 1, the computed diffusivity profiles are very similar. The reduction in the computed diffusivities required to match the reduced profile gradients is striking between ψ_N of 0.8 and 0.94, indicating that transport is improving inside the H-mode barrier. In effect, the H-mode barrier is simply growing inward. The particle transport appears to be reduced in the SOL for $\psi_N > 1$ (Figure 1a), but additional cases are needed to confirm this since the density is quite low. We note that while these simulations were conducted with deuterium alone, the inclusion of carbon does not alter the conclusions[8].

Stability calculations have shown that the NSTX ELM suppression is caused by broadening of the pressure profile and the corresponding edge bootstrap current, owing mainly to the modification of the density profile[6]. This broadening of the pressure profile is illustrated in Figure 2. The effect of li coatings on the total

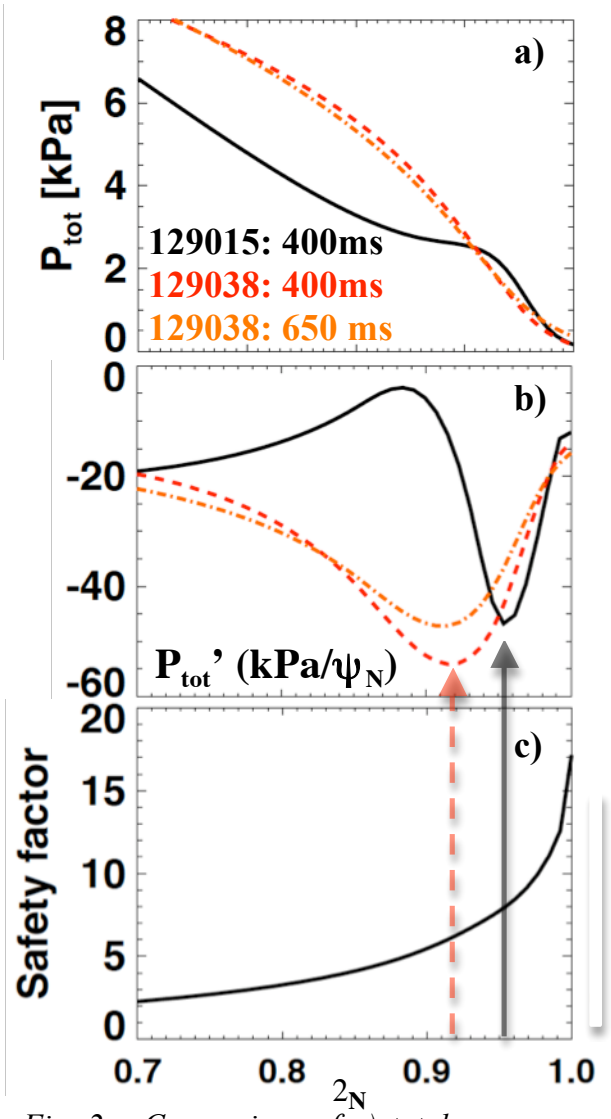

Fig. 2 – Comparison of a) total pressure, b) P', and c) safety factor for pre-li (solid black) and post-li (dashed red, dash-dot orange) time slices.

pressure profile from a kinetic equilibrium fitting procedure[9] is shown in Figure 2a. Figure 2b shows that the peak pressure gradient moves inward from ψ_N~0.95 to ψ_N~0.92 after li coatings. Note that the peak pressure gradient value is comparable to or higher than the pre-li value; the main difference is that it was moved farther from the separatrix, which is generally stabilizing to edge current-driven kink/peeling modes. Figure 2c shows that the peak pressure gradient also moved to a region of lower magnetic shear, which is also stabilizing in this case. The connection between the pressure gradient and the edge current in the stability calculations is through the bootstrap current, which can comprise a substantial portion of the parallel current. Here the bootstrap current is computed from a neoclassical formula[10], since no direct measurement exists in NSTX. While this represents the largest uncertainty in this analysis procedure, we note that a measurement of this bootstrap current with a lithium beam in DIII-D agreed reasonably well in an L-mode and an H-mode discharge[11]. Nonetheless this uncertainty motivates the testing of other theories[12] of ELM suppression in discharges with li wall coatings.

More specifically, calculations with the PEST[13] and ELITE[14, 15] codes have confirmed that the post-lithium discharge pressure profiles were farther from the stability boundary than the reference pre-lithium discharges, which were relatively close to the kink/peeling boundary. Indeed low-n (n=1-5) pre-cursors were observed prior to the ELM crashes in the reference discharges, in semi-quantitative agreement with the PEST and ELITE results[6]. The link between the lithium wall coatings and the ELM suppression is shown schematically in Figure 3.

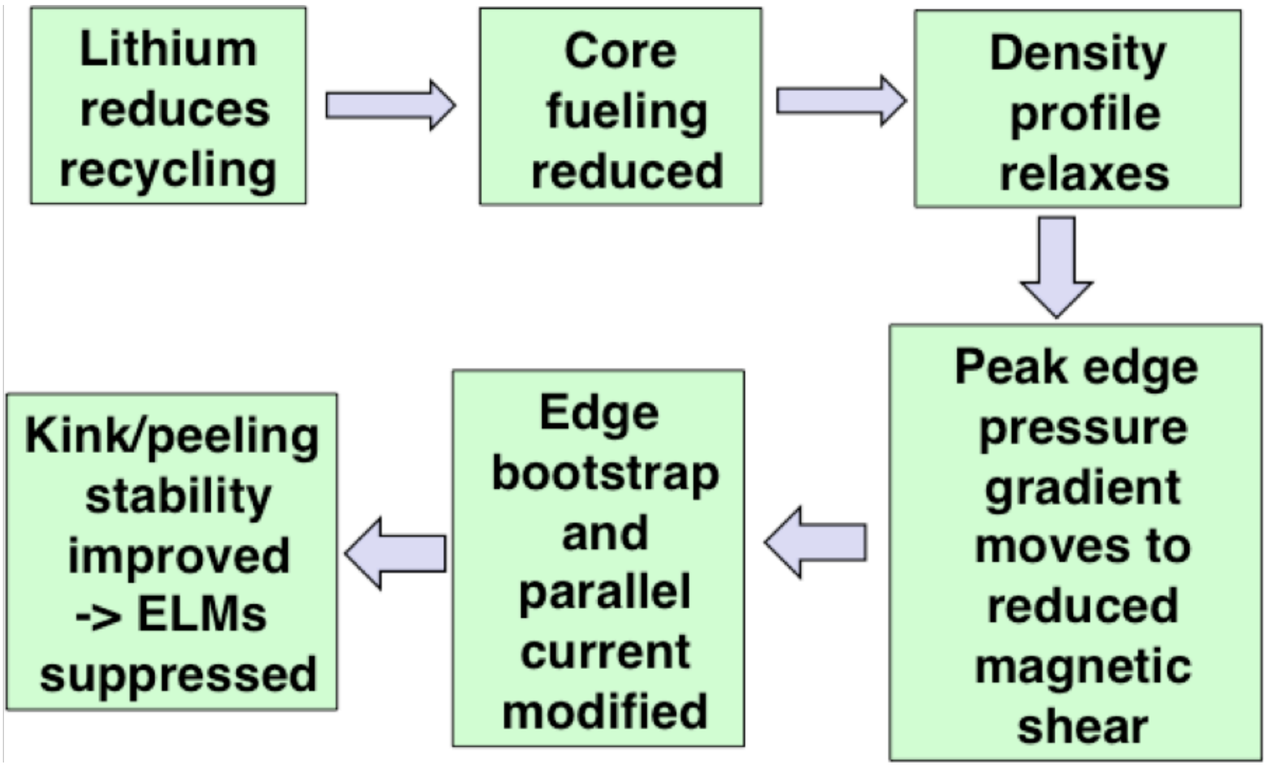

Fig. 3 – flow chart describing effects of lithium leading to ELM suppression

Clearly the use of li wall coatings is not a panacea in this context. Although the energy confinement improves substantially, true ELM-free H-mode is not a stationary state. Left unabated, these ELM-free discharges would otherwise suffer radiative collapse from carbon and high-Z impurity accumulation. At present we are employing pulsed 3-d magnetic fields to trigger ELMs for impurity control and radiated power control[16-18]. While the triggered ELM size is not an issue for present NSTX operation, and can be reduced, e.g. operation at modestly higher q95, the present ELMs with a 5% fractional energy loss project to unacceptable transient heat loads in future devices. We have recently also evaluated the use of low amplitude, short duration 3-D fields below the ELM triggering threshold as a mechanism to increase particle transport[19]. Other techniques, e.g. the use of rf heating to purge core impurities, are being evaluated for use in conjunction with ELM pace-making by 3D fields. Finally we are also exploring methods to reduce the impurity source from physical sputtering, e.g. through high flux expansion 'snowflake' divertor topologies that result in reduced heat flux and impurity content[20,21].

This research was sponsored in part by the U.S. Dept. of Energy under contracts DE-AC05-00OR22725, DE-AC02-09CH11466, and DE-FC02-04ER54698. The efforts of the NSTX operations staff and the computer support staff are gratefully acknowledged.

References

1 H. W. Kugel, et. al., *Phys. Plasma* **15** (2008) 056118.
2 M. G. Bell, et. al., *Plasma Phys. Contr. Fusion* **51** (2009) 124054.
3 S. Ding, et. al., *Plasma Phys. Contr. Fusion* **52** (2010) 015001.
4 D. K. Mansfield, et. al., *J. Nucl. Materials* **390-391** (2009) 764.
5 R. Maingi, et. al., *Proc. of the 2009 EPS Conference on Plasma Physics and Controlled Fusion, Sofia, Bulgaria, June 29-July 3* (2009) paper P2.175.
6 R. Maingi, et. al., *Phys. Rev. Letts.* **103** (2009) 075001.
7 R. Schneider, et. al., *Contrib. Plasma Physics* **46** (2006) 3.
8 J. M. Canik, et. al., *J. Nucl. Mater.* (2010) submitted.
9 T. H. Osborne, et. al., *J. Phys.: Conf. Series* **123** (2008) 012014.
10 O. Sauter, et. al., *Phys. Plasma* **6** (1999) 2834.
11 D. M. Thomas, et. al., *Phys. Rev. Lett.* **93** (2004) 065003.
12 L. E. Zakharov, et. al., *J. Nucl. Mater.* **363-365** (2007) 453.
13 R. Grimm, et. al., *Methods Comput. Phys.* **16** (1976) 253.
14 H. R. Wilson, et. al., *Phys. Plasma* **9** (2002) 1277.
15 P. B. Snyder, et. al., *Phys. Plasma* **9** (2002) 2037.
16 J. M. Canik, et. al., *Phys. Rev. Letts.* **104** (2010) 045001.
17 J. M. Canik, et. al., *Nucl. Fusion* **50** (2010) 034012.
18 J. M. Canik, et. al., *Nucl. Fusion* **51** (2010) 064016.
19 J. M. Canik, et. al., *this conference* (2010) paper P2.123.
20 V.A. Soukhanovskii, et. al., *J. Nucl. Mater.* (2010) submitted.
21 V.A. Soukhanovskii, et. al., *this conference* (2010) paper P2.161.